AFRL-PR-WP-TP-2006-251

ELECTRON-IMPACT DISSOCIATIVE IONIZATION OF ETHYLENE (POSTPRINT)

S. Popović, S. Williams, and L. Vušković

FEBRUARY 2006

Approved for public release; distribution is unlimited.

STINFO COPY

PROPULSION DIRECTORATE
AIR FORCE MATERIEL COMMAND
AIR FORCE RESEARCH LABORATORY
WRIGHT-PATTERSON AIR FORCE BASE, OH 45433-7251

REPORT DOCUMENTATION PAGE

Form Approved
OMB No. 0704-0188

1. REPORT DATE *(DD-MM-YY)*	2. REPORT TYPE	3. DATES COVERED *(From - To)*
February 2006	Journal Article Postprint	09/21/2004 – 11/03/2005

4. TITLE AND SUBTITLE
ELECTRON-IMPACT DISSOCIATIVE IONIZATION OF ETHYLENE (POSTPRINT)

5a. CONTRACT NUMBER
In-house

5b. GRANT NUMBER

5c. PROGRAM ELEMENT NUMBER
61102F

6. AUTHOR(S)
S. Popović and L. Vušković (Old Dominion University)
S. Williams (AFRL/PRAS)

5d. PROJECT NUMBER
2308

5e. TASK NUMBER
AI

5f. WORK UNIT NUMBER
01

7. PERFORMING ORGANIZATION NAME(S) AND ADDRESS(ES)
Old Dominion University
Department of Physics
Norfolk, VA 23529

Propulsion Sciences Branch (AFRL/PRAS)
Aerospace Propulsion Division
Propulsion Directorate
Air Force Research Laboratory, Air Force Materiel Command
Wright-Patterson Air Force Base, OH 45433-7251

8. PERFORMING ORGANIZATION REPORT NUMBER
AFRL-PR-WP-TP-2006-251

9. SPONSORING/MONITORING AGENCY NAME(S) AND ADDRESS(ES)
Propulsion Directorate
Air Force Research Laboratory
Air Force Materiel Command
Wright-Patterson AFB, OH 45433-7251

10. SPONSORING/MONITORING AGENCY ACRONYM(S)
AFRL-PR-WP

11. SPONSORING/MONITORING AGENCY REPORT NUMBER(S)
AFRL-PR-WP-TP-2006-251

12. DISTRIBUTION/AVAILABILITY STATEMENT
Approved for public release; distribution is unlimited.

13. SUPPLEMENTARY NOTES

Journal article published in Physical Review A, Vol. 73 (2006), The American Physical Society, publisher.

PAO case number: AFRL/WS 05-2667; Date cleared: 17 Nov 2005.

14. ABSTRACT
The ionization rates of the electron-impact ionization and dissociative ionization of ethylene for two typical cases: thermal plasmas with an electron temperature in the range between 1000 and 24,000 K; and nonthermal plasmas with the reduced electric field in the range between 10 and 200 Td are presented. Electron-impact dissociative ionization rates were calculated for 11 fragment ions of ethylene in the case of low temperature thermal plasma, and in a case of nonthermal ionized mixture of argon and ethylene. Dissociative ionization cross sections were calculated using a semiempirical binary-encounter bethe (BEB) model [Y. K. Kim and M. E. Rudd, Phys. Rev. A 50, 3954 (1994)], with each of the four most dominant fragments, $C_2H_4^+$, $C_2H_3^+$, $C_2H_2^+$, and H^+, being associated with a single molecular orbital. Calculated cross sections are used in this analysis due to the fact that the existing experimental data are the least accurate in the threshold region and the calculated results can improve the accuracy in that region. Also, the procedure may be extended to molecules for which experimental data are not available.

15. SUBJECT TERMS
Plasma enhanced combustion, ethylene, kinetics models, CFD chemistry models, reduced mechanism, reduced chemistry

16. SECURITY CLASSIFICATION OF:			17. LIMITATION OF ABSTRACT:	18. NUMBER OF PAGES	19a. NAME OF RESPONSIBLE PERSON (Monitor)
a. REPORT	b. ABSTRACT	c. THIS PAGE			Dr. Skip Williams
Unclassified	Unclassified	Unclassified	SAR	14	19b. TELEPHONE NUMBER *(Include Area Code)* N/A

Standard Form 298 (Rev. 8-98)
Prescribed by ANSI Std. Z39-18

Electron-impact dissociative ionization of ethylene

S. Popović,[1,*] S. Williams,[2,†] and L. Vušković[1,‡]
[1]*Department of Physics, Old Dominion University, Norfolk, Virginia 23529, USA*
[2]*Air Force Research Laboratory, Propulsion Directorate, WPAFB, Ohio 45433, USA*
(Received 3 November 2005; published 13 February 2006)

The ionization rates of the electron-impact ionization and dissociative ionization of ethylene for two typical cases: thermal plasmas with an electron temperature in the range between 1000 and 24 000 K; and nonthermal plasmas with the reduced electric field in the range between 10 and 200 Td are presented. Electron-impact dissociative ionization rates were calculated for 11 fragment ions of ethylene in the case of low temperature thermal plasma, and in a case of nonthermal ionized mixture of argon and ethylene. Dissociative ionization cross sections were calculated using a semiempirical binary-encounter bethe (BEB) model [Y. K. Kim and M. E. Rudd, Phys. Rev. A **50**, 3954 (1994)], with each of the four most dominant fragments, $C_2H_4^+$, $C_2H_3^+$, $C_2H_2^+$, and H^+, being associated with a single molecular orbital. Calculated cross sections are used in this analysis due to the fact that the existing experimental data are the least accurate in the threshold region and the calculated results can improve the accuracy in that region. Also, the procedure may be extended to molecules for which experimental data are not available.

DOI: 10.1103/PhysRevA.73.022711 PACS number(s): 34.80.Gs, 34.80.Ht, 52.20.Fs, 52.20.Hv

I. INTRODUCTION

Chemical kinetic models of ignition and combustion under plasma conditions require reliable data on total and on dissociative ionization processes. Total electron-impact ionization rates are known rather accurately for atmospheric or small hydrocarbon molecules, but very few data exist on more complex hydrocarbons or on dissociative ionization rates and the production of hydrocarbon fragment ions. In the case of more complex hydrocarbons, where the experimental database is limited to a few molecular species, calculation techniques with advanced predictability, taking into account the current knowledge of the collision cross sections, are very much needed. In addition, ionized fragments of ethylene are found in the interstellar space and in the planetary ionospheres. However, our goal is to understand the dissociative ionization process in low electron energy regimes of electric discharge plasmas.

Dissociative ionization (DI) processes are very important in plasmas and DI processes involving hydrocarbons will be very important for new applications of plasma to enhance combustion. Rates for the generation of radical ions by the electron impact on hydrocarbon molecules are an important subset of data for the chemical kinetic modeling of a wide range of the plasma-assisted processes involving hydrocarbons. Besides the obvious impact on ion and neutral composition, radical ion generation processes define charge particle balance and electron temperature in molecular plasmas. These data are largely unavailable and are usually derived indirectly, by elimination, rather than by experiment or calculation. One of the problems with the current experimental data on fragmentary ionization processes is that the practical application usually requires a behavior of cross-section data at low energies, near the threshold, where some of the available experimental methods are the least accurate [1]. More accurate experimental techniques [2] have not been used to study ethylene. On the other hand, recently developed calculations give more or less correct values of the total ionization cross section [3–5], but are still unable to produce full data sets for fragment ion generations.

In this paper, the quantitative analysis of the electron-impact ionization of ethylene, where the partial ionization cross sections for fragment generation are correlated with the molecular structure is presented. Successful completion of this analysis may lead to new semiempirical calculation models that combine the experimental data on molecular structure and fragmentation processes with the binary-encounter-bethe model [3–5] to produce reliable fragmentary ionization rates for an application in discharges involving hydrocarbons.

II. TOTAL CROSS SECTION FOR ELECTRON-IMPACT IONIZATION OF ETHYLENE

Kim and co-workers [3–7] have provided a useful formula for electron-impact ionization using a theory referred to by these authors as the binary-encounter-bethe (BEB) model.

The basic formula for the ionization cross section per molecular orbital is [7],

$$\sigma_{BEB} = \frac{S}{t + \frac{u+1}{n}}\left[\frac{Q\ln t}{2}\left(1-\frac{1}{t^2}\right) + (2-Q)\left(1-\frac{1}{t}-\frac{\ln t}{t+1}\right)\right], \tag{1}$$

where $t=T/B$, $u=U/B$, $S=4pa_0^2N(R/B)^2$, $a_0=0.529\ 18$ Å, $R=13.6057$ eV, B is the binding energy, U is the orbital kinetic energy, N is the electron occupation number, Q is the dipole constant, $n=1$ for neutral molecules, and $n=2$ for the

*Email address: popovic@physics.odu.edu
†Email address: skip.williams@wpafb.af.mil
‡Email address: vuskovic@physics.odu.edu

TABLE I. HOMO binding energy and ionization energy for $C_4H_4^+$. Experimental value for the ionization energy of C_2H_4 is 10.51 eV.

Model	HOMO binding energy (eV)	Ionization energy (eV)
RHF/6-31G(d)	10.19	8.78
RHF/6-311G(2df)	10.37	8.90
B3LYP/6-311+G(3df,2p)	7.69	10.33
G1	10.21	10.59
G2	10.26	10.58
G2(MP2)	10.26	10.59

singly charged molecular ion. The dipole constant Q is defined [6] in terms of the continuum dipole oscillator strength df/dW,

$$Q = \frac{2}{N}\int \frac{B}{B+W}\frac{df}{dW}dW, \tag{2}$$

where W is the kinetic energy of the ionized electron. By assuming that a simple form for df/dW, namely, $df/dW \sim (B\text{-}W)^{-2}$, which approximately describes the asymptotic behavior of the oscillator strength in hydrogen atoms in the ground state, reliable differential ionization cross sections can be obtained for molecules with simple shell structures including highly symmetrical hydrocarbon molecules, such as ethylene. In addition, this assumption results in $Q=1$ which greatly simplifies the calculation of the cross section.

The total electron-impact ionization cross section is then obtained by summation over all occupied molecular orbitals. In order to obtain the parameters relating to the molecular orbitals, *ab initio* quantum mechanical calculations are performed. One difficulty encountered in performing these calculations for hydrocarbon ions is the accurate calculation of low lying electronic states; however, the BEB model only requires information regarding the ground state wave function. Calculations have been carried out at the Hartree-Fock level of theory with Gaussian basis sets [8] in order first to calculate the molecular geometry. The resulting wave functions were varied to determine if it corresponded to the lowest-lying electronic state—and if not, the multiplicity or electron configuration was adjusted so as to yield the ground state.

Higher-level calculations including the G2(MP2) method of GAUSSIAN 98 [8] were also performed but did not change the results appreciably (see Table I) implying that the use of the higher-level calculations are not warranted in the case of the highest occupied molecular orbital (HOMO) binding energy. The observation that Hartree-Fock wave functions are adequate has been observed for many molecules [3–5,7]. The orbital parameters B, U, and N are obtained by the quantum chemistry calculations and are listed in Table II.

The molecular orbital constants N, B, and U can easily be calculated using standard molecular wave function codes. However, BEB cross sections at low temperature are sensitive to the lowest binding energy and the experimental vertical ionization potential should be used if available, unless the calculated value of the binding energy has included the effect of electron correlation. Therefore, the average measured ionization potential for ethylene and the appearance potentials for fragments ions have been presented in Table III. The mean fraction of the total cross section was taken over the energy range 10–200 eV.

TABLE II. Molecular orbitals (MO), electron binding energy (B), orbital kinetic energy (U), and electron occupation number (N). B and U values are obtained using the G2 method.

MO	B (eV)	U (eV)	N
$1a_g$	305.64	435.74	2
$1b_{1u}$	305.59	436.19	2
$2a_g$	28.12	40.52	2
$2b_{1u}$	21.59	33.55	2
$1b_{2u}$	17.48	25.23	2
$3a_g$	16.03	34.71	2
$1b_{3g}$	13.80	28.59	2
$1b_{3u}$	10.26	25.83	2

Total ionization cross-section data for ethylene are given in Fig. 1 for the energy range that is relevant for plasma kinetic studies, that is from the threshold energy to 100 eV. The two sets of results calculated using the HOMO binding energy and using the experimental ionization potential, are in fairly good agreement. The discrepancy between calculated and experimental data is still substantial. Early measurements of absolute total ionization cross section by Rapp and Englander-Golden [10] are in good agreement with calculations around the threshold energies, but higher by about 25% at higher energies (>40 eV). Experimental results of Nishimura and Tawara [11] are in rather good agreement with calculations over the full energy range, especially near the

TABLE III. Mean fraction of the total cross section for the observable fragment ions of C_2H_4. (* obtained by electron-impact method exclusively).

Fragment ion	Appearance potential (eV) [6]*, [9]	Evaluated appearance potential (eV)	Mean fraction of total cross-section [1]	Relative uncertainty
$C_2H_4^+$	10.51	10.51	0.336	±6%
$C_2H_3^+$	13.10-13.52	13.06	0.233	±9%
$C_2H_2^+$	13.14	13.20	0.212	±3%
C_2H^+	18.70-19.20	19.22	0.039	±24%
C_2^+	24.50	24.06	0.013	±26%
CH_4^+	18.66	18.82	…	
CH_3^+	16.95	16.96	0.0025	±17%
CH_2^+	17.82	17.95	0.0482	±13%
CH^+	17.68	17.76	0.0201	±31%
C^+	18.30	17.37	0.0129	±28%
H_2^+	22.40	23.04	0.0054	±26%
H^+	18.66	18.41	0.0773	±28%

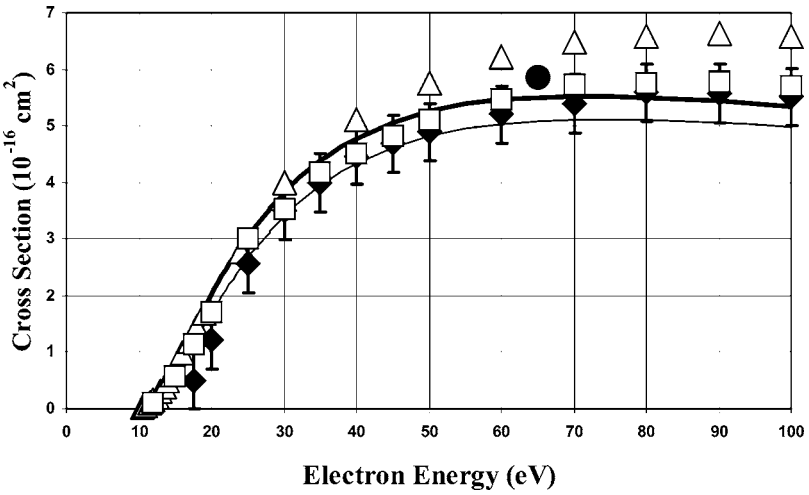

FIG. 1. Total cross section for electron-impact ionization of ethylene. Experiment: ◆, Ref. [1]; □, Ref. [11]; △, Ref. [10]; ●, Ref. [12]. Calculation: thick solid line, BEB calculation with the binding energies of the highest three OMO substituted by the appearance potentials of $C_2H_4^+$, $C_2H_3^+$, and $C_2H_2^+$, respectively; thin solid line, calculation using computed binding energies and experimental ionization energy for HOMO.

threshold. The discrepancy is reduced by substituting the binding energy of several higher occupied molecular orbitals with the appropriate experimental appearance potentials for certain ion fragments. Using this approach, the agreement between the experimental and calculated data below 70 eV is achieved with the overall uncertainty of 5%.

Values for the absolute total cross section at high energies obtained by Tian and Vidal [1] are in a good agreement with other data in the energy range between 25 and 60 eV. The values near the threshold are substantially lower due to a experimental normalization procedure based on the argon ion counting. Ethylene fragment ions with a low appearance potential (binding energy) were not possible to observe in that experiment because of the high value of argon ionization potential, which is 15.756 eV. Except for the systematic error near the threshold for ions with lower appearance potentials, data at energies around 50 eV give very good foundation for the analysis of ethylene ion fragmentation. Finally, the value of 5.86×10^{-16} cm^2 at 70 eV, obtained using an additive formula of Ref. [12] is also in a fairly good agreement with the experiment and calculation.

III. PARTIAL IONIZATION CROSS SECTIONS

In this section the possibility to predict the fragmentation branching fractions based on the molecular structure is explored. This section outlines a process to reproduce the experimental results on fragmentation by molecular structure reactant-product analysis. If that exercise proves successful, we could proceed with fragmentation analysis for heavier hydrocarbons.

Tian and Vidal [1] have published tabulated values of dissociative ionization cross sections for the electron impact on ethylene in the energy range between 17.5 and 600 eV. There are three distinctive groups of 12 possible ionic fragments, $C_2H_n^+$ (n=0, 1, 2, 3, and 4), CH_n^+ (n=0, 1, 2, 3, and 4), and H_n^+ (n=1,2). Tian and Vidal [1] were able to observe 11 of them. In Table III are given their appearance potentials compiled from ion energetics reference data [6], and relative contributions of the particular ion products evaluated from the experimental data [1] over the electron energy range 50–600 eV.

An inspection of Table III reveals that one-third of the total cross section belongs to the nondissociative ionization by electron impact

$$e^- + C_2H_4 \rightarrow C_2H_4^+ + e^- + e^-. \quad (3)$$

Most probable experimental electron-impact dissociative ionization processes produce fragment ions without breaking carbon bonds, namely,

$$e^- + C_2H_4 \rightarrow C_2H_3^+ + H + e^- + e^- \quad (4)$$

and

$$e^- + C_2H_4 \rightarrow C_2H_2^+ + H_2 + e^- + e^-. \quad (5)$$

Taken together, the electron-impact ionization processes leading to the group $C_2H_n^+$ account for more than 80% of ion products. Other important processes are

$$e^- + C_2H_4 \rightarrow H^+ + C_2H_3 + e^- + e^- \quad (6)$$

and

$$e^- + C_2H_4 \rightarrow CH_2^+ + CH_2 + e^- + e^-. \quad (7)$$

Only reaction (7) involves carbon bond breaking. It is interesting to note that fragment ions CH_4^+ and CH_3^+ have very low ionization cross sections, since their formation requires carbon bond breaking and redistribution of hydrogen atoms. CH_4^+ is not observed in the experiment [1], in spite of its relatively low appearance potential. We can conclude that dominant fragment ions are those that do not require carbon bond breaking.

A. $C_2H_n^+$ ions

Since the formation of the ethylene ion, $C_2H_4^+$, does not involve any bond breaking, it is natural to assume that the removed electron was associated with HOMO. Therefore, we first inspect the relation between the experimental nondissociative ionization cross section for electron impact on C_2H_4 and the calculated partial ionization cross section associated with the HOMO with its binding energy substituted by the vertical ionization potential IP=10.51 eV. The results are given in Fig. 2 for the electron energy from the threshold to

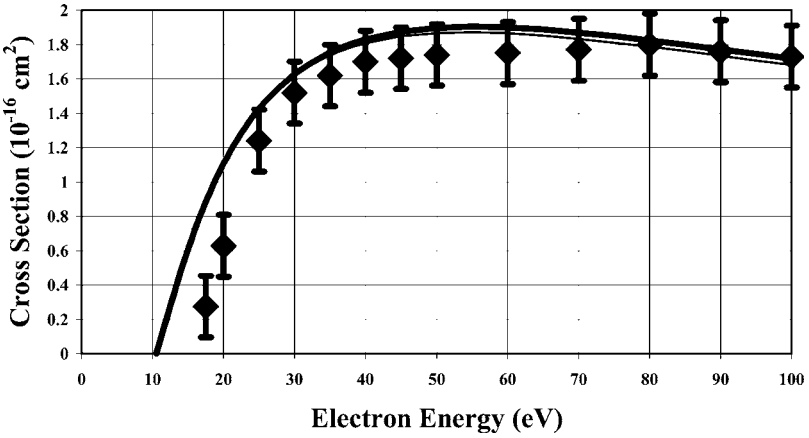

FIG. 2. Partial ionization cross section for $C_2H_4^+$ formation. Experiment: ♦, Ref. [1]. Calculation: thick solid line, calculation based only on HOMO with the binding energy equal to the vertical ionization potential (AP=10.51 eV); thin solid line, calculation using computed binding energy for HOMO.

100 eV. The agreement is better than 5% at energies above 50 eV, which is comparable to the uncertainties of calculated values, mostly due to the uncertainty of the binding energy (2%) and uncertainty of the orbital kinetic energy U (2.5%), based on more than a dozen models tested up to the level of G2. At energies from the threshold to 50 eV we have more reason to believe that HOMO ionization cross-section values are more reliable than the experimental data, since the experiment cannot record the threshold values, and the experimental error remains high up to about 50 eV. It has been mentioned earlier that the experiment [1] could not reproduce the threshold values correctly, since the appearance potential for $C_2H_4^+$ is lower than the ionization potential of argon, which served as the carrier gas.

Results for other two important ion fragments from the same group, $C_2H_3^+$, and $C_2H_2^+$, are given in Figs. 3 and 4, respectively. Figure 3 shows results of the calculations of partial ionization cross section for the $1b_{3g}$ orbital together with experimental data for the fractional ionization cross section for the $C_2H_3^+$ ion fragment. The cross sections calculated using the orbital parameters obtained at the HF/6-31G(d) level of theory yielding for the $1b_{3g}$ MO a binding energy B of 13.66 eV are in good agreement with the experimental data at an energy above 50 eV. Higher levels of Hartree-Fock techniques give slightly higher values of binding energy, up to 13.80 eV. When the binding energy for this orbital is substituted by the average experimental appearance potential, AP=13.33 eV for $C_2H_3^+$, the corresponding partial ionization cross section is slightly increased. Taking into account the uncertainties in the experimental and calculated data, the two calculations can be considered almost as identical. The agreement between the two calculations suggests that the partial ionization cross section for the $1b_{3g}$ orbital is an adequate approximation for the dissociative ionization leading to vinyl ion $C_2H_3^+$.

Quantitative agreement between the empirical approach and MO calculation, starts to break down at the next occupied orbital, $3a_g$. Remedy for this particular case is to substitute the binding energy of the orbital $3a_g$, with the appearance potential for the $C_2H_2^+$, as in the many cases of total ionization cross sections [6]. As seen in Fig. 4, this approach gives a quite accurate reproduction of cross sections both in the threshold region and at higher energies, where it could be tested by the experimental data. Partial ionization cross sections corresponding to the next available molecular orbital, $3a_g$, is about 40% lower than the experimental dissociative ionization cross section of the $C_2H_2^+$ ion fragment. The large difference between the calculated binding energy of this orbital (15.97 eV) and the average experimental appearance potential (13.17 eV) is responsible for the large differences shown in Fig. 4 between the two calculations.

B. Hydrogen ions

A similar situation is found in the case of a H^+ fragment ion, as seen in Fig. 5, where the discrepancy between empirical calculation and the experiment is more profound,

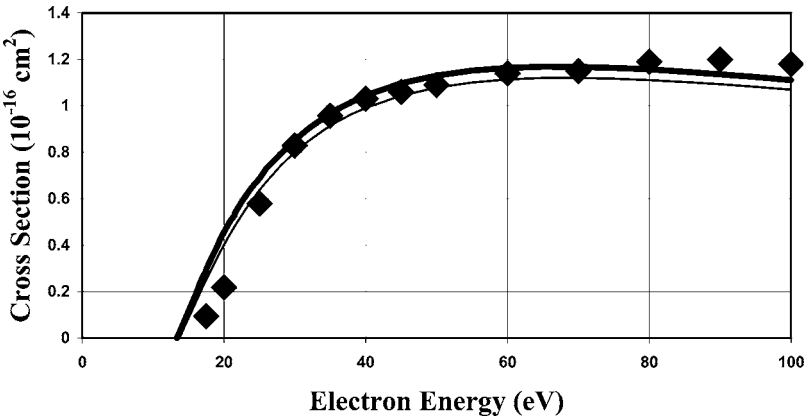

FIG. 3. Partial ionization cross section for the production of $C_2H_3^+$ fragment ion. Experiment: ♦, Ref. [1]. Calculation: thick solid line, BEB based on the same MO with AP=13.06 eV instead of binding energy of 13.80 eV; thin solid line, BEB based only on the MO $1b_{3g}$.

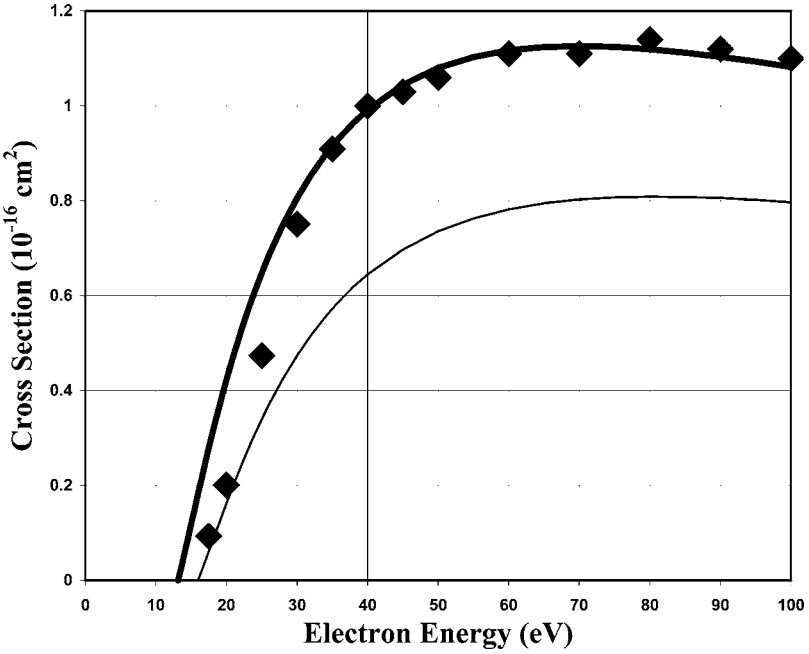

FIG. 4. Partial ionization cross section for the production of $C_2H_2^+$ fragment ion. Experiment: ♦, Ref. [1]. Calculation: thick solid line, BEB based only on the MO $3a_{1g}$ with an appearance potential of 13.20 eV; thin solid line, BEB based on MO $3a_{1g}$ with a calculated binding energy of 16.03 eV.

but still rather close to the frame of experimental error. However, the use of the binding energy for the $1b_{2u}$ MO from Table II would lead to a large overestimate of this cross section. Therefore, the binding energy for the same hydrogen-bonding orbit $1b_{2u}$ was substituted by the appearance potential of H^+.

C. Other ions

Cross sections for dominant ion species $C_2H_4^+$, $C_2H_3^+$, $C_2H_2^+$, and H^+ can each be associated with a single molecular orbital and calculated using the values of appearance potentials instead of the binding energy. These cross sections are then in very good agreement with the experiment. However, this approach is not sufficient, since it is obvious from Tables II and III that there cannot be a one-on-one correspondence between the molecular orbitals and ion fragments. Moreover, calculated binding energies differ considerably from the appearance potentials of particular ion fragments.

The sum of dissociative ionization cross sections for four main fragment ions, $C_2H_4^+$ (see Fig. 2), $C_2H_3^+$ (see Fig. 3), $C_2H_2^+$ (Fig. 4), and H^+ (Fig. 5), calculated using their appearance potentials instead of the calculated binding energies of the assigned MO, constitute more then 80% of the total ionization cross section for ethylene. The remaining 20% is distributed between all other fragment ions. In Fig. 6, we compare the sum of BEB cross sections of the next two occupied orbits of C_2H_4, $2b1_u$, and $2a_g$ with the sum of the experimental cross sections of all other observable ions, C_2H^+, C_2^+, CH_3^+, CH_2^+, CH^+, C^+, and H_2^+. Here the ethynyl radical ion C_2H^+, dicarbon ion C_2^+, and hydrogen molecular ion were associated with the $2b_{1u}$ orbital, and the methyl radical ion CH_3^+, methylene ion CH_2^+, methylidyne ion CH^+, and carbon ion C^+, were associated with the $2a_g$ orbital. Appearance potentials for these ion fragments are higher than the ionization potential of argon, and the experimental data from Ref. [1] should be accurate within the stated error of 10%. This is reflected in the fact that the present calculation and experiment [1] are in much better agreement near the threshold.

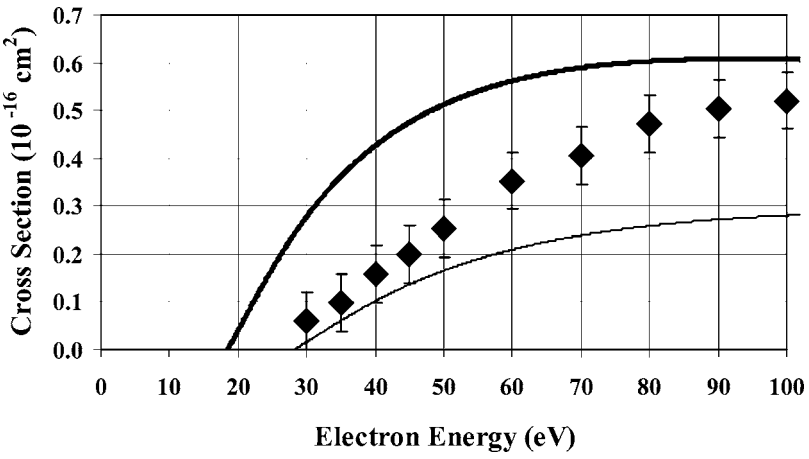

FIG. 5. Partial ionization cross section for H^+ fragment ion. Experiment: ♦. Ref. [1]. Calculation: thick solid line, BEB using only MO $2a_g$ with AP=22.3 eV instead of binding energy; thin solid line, BEB based on MO $2a_g$ with a calculated binding energy of 28.12 eV.

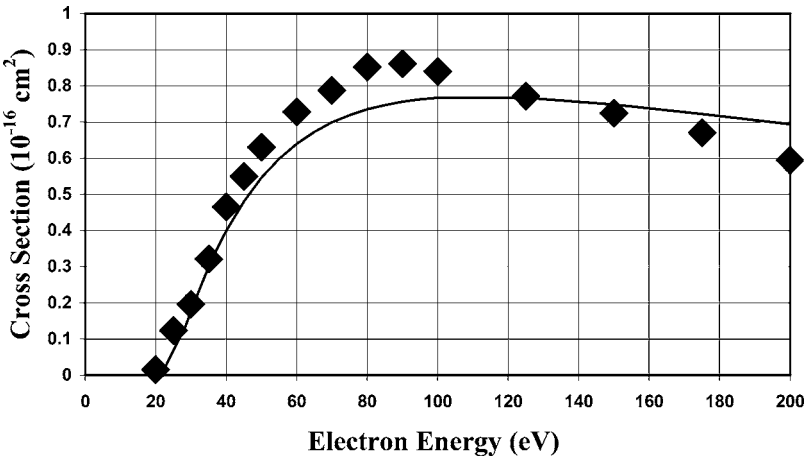

FIG. 6. Total ionization cross section of the remaining observable fragment ions (CH_3^+, CH_2^+, CH^+, C^+, C_2H^+, C_2^+, and H_2^+). Experiment: ♦, Ref. [1]. Calculation: thin solid line, BEB using the $2b_{1u}$ and $2a_g$ MO with corresponding appearance potentials.

IV. IONIZATION RATES

While the near-threshold value cross sections are not particularly meaningful in the astrophysical plasmas where the ionization processes are carried on by more energetic particles, they are very important in the laboratory processing plasmas. Since the electrons capable to ionize are in the tail of their energy distribution, the threshold energy and absolute value of the cross section for each fragment ion are critical for determining the ionization rates in typical plasmas. In evaluating the ionization rates for the dissociative ionization of ethylene in discharge plasmas, two distinct situations are considered. The first case assumes that the electrons in the discharge are in equilibrium, with their temperature defined by the Maxwellian energy distribution. The second case assumes the discharge in a lean mixture of ethylene and argon, where electron energy distribution function is defined by the reduced electric field E/N, in the discharge dominated by argon collision processes. Both cases are characterized by relatively low average electron energy, order of 1 to 2 eV, and are therefore sensitive to the near-threshold values of ionization cross sections. Both cases are typical of laboratory-scale plasma.

Ionization rates for thermal plasmas are given in Table IV and have been obtained by convoluting the computational cross section data with a Maxwellian electron distribution fuction. For the electron temperature range from 1000 to 24 000 K, the ionization rate coefficients are well described by an Arrhenius form.

In the more frequent case of nonthermal plasmas, the electron temperature has a somewhat ambiguous meaning of the average electron energy, and a more appropriate parameter defining a particular electron energy distribution function is the reduced electric field E/N. Ionization rates of fragment ions at 10, 50, 100, and 200 Td (1 Td $=10^{-17}$ V cm^2) in a lean mixture of ethylene with argon, are given in Table V. It is interesting to note that the dominance of the fragment ions with carbon bonds preserved is much more pronounced. All other fragment ions appear in traces at low E/N. At high E/N, the appearance of C_2H^+, CH_2^+, and H^+ can be counted in parts of a percent.

The experimental cross section values of the most abundant fragment ions [1] near threshold cannot be used due to the systematic error for product channels with threshold energies below the ionization potential of argon as previously discussed. Therefore, in order to compare the ionization rates obtained from the BEB model calculation to those derived from the experimental data, the experimental points for electron energies below 25 eV were eliminated and approximated by linearly interpolating the value of the cross section from 25 to 10.51 eV. The maximum difference between the ionization rate coefficients derived from the modified experimental and calculated cross sections is about 35% at high temperatures (above 10 000 K) and high E/N (above 10 Td). Based on these results, the values of ionization recorded in Tables IV and V are accurate to 35% for the ions with appearance potentials below the ionization potential of argon, i.e., the major product channels $C_2H_4^+$, $C_2H_3^+$, and $C_2H_2^+$.

For fragment ions with appearance potentials above the ionization potential of argon, the experimental values near threshold are reliable. In these cases, the ionization rates were calculated from the experimental data using a recurrent polynomial formula in the threshold region to make the data continuous. This procedure results in differences between the ionization rate coefficients derived from the modified experi-

TABLE IV. Fitted Arrhenius parameters ($k=Ae^{B/T_e}$) for partial ionization rates of ethylene fragment ions in thermal discharge plasmas.

Fragment ions	A (10^{-8} cm^3 s^{-1})	B (1000 K)
$C_2H_4^+$	1.7107	125.47
$C_2H_3^+$	1.0514	158.12
$C_2H_2^+$	0.9632	156.18
C_2H^+	0.1661	225.01
C_2^+	0.02716	308.88
CH_3^+	0.009342	204.36
CH_2^+	0.1771	233.10
CH^+	0.08087	264.67
C^+	0.009213	214.91
H_2^+	0.01985	262.80
H^+	0.3957	260.53

TABLE V. Partial ionization rates of ethylene fragment ions in a very lean mixture of ethylene with weakly ionized argon in units of ($cm^3\ s^{-1}$) for different E/N value.

Fragment ions	10 (Td)	50 (Td)	100 (Td)	200 (Td)
$C_2H_4^+$	9.63×10^{-14}	8.02×10^{-13}	1.62×10^{-12}	4.78×10^{-12}
$C_2H_3^+$	9.04×10^{-17}	4.51×10^{-14}	2.27×10^{-13}	1.09×10^{-12}
$C_2H_2^+$	1.36×10^{-16}	4.82×10^{-14}	2.28×10^{-13}	1.06×10^{-12}
C_2H^+	2.11×10^{-30}	1.14×10^{-17}	9.68×10^{-16}	1.75×10^{-14}
C_2^+	…	8.93×10^{-23}	1.44×10^{-18}	2.53×10^{-16}
CH_3^+	5.42×10^{-28}	3.35×10^{-18}	1.44×10^{-16}	1.90×10^{-15}
CH_2^+	2.68×10^{-27}	3.69×10^{-17}	1.73×10^{-15}	2.39×10^{-14}
CH^+	…	1.86×10^{-19}	9.59×10^{-17}	3.44×10^{-15}
C^+	1.04×10^{-30}	1.77×10^{-18}	1.07×10^{-16}	1.82×10^{-15}
H_2^+	…	1.50×10^{-20}	1.11×10^{-17}	4.84×10^{-16}
H^+	…	3.77×10^{-19}	2.59×10^{-16}	1.16×10^{-14}

mental and calculated cross sections is about 50–70 % for the ionization rates for the minor product channels.

V. CONCLUSION

Ionization rates of electron-impact ionization and dissociative ionization of ethylene for two typical cases: thermal plasmas with electron temperature in the range between 1000 and 24 000 K; and nonthermal plasmas with the reduced electric field in the range between 10 and 200 Td have been calculated. The values obtained for ionization rates are based on the calculated absolute dissociative ionization cross sections using the binary-encounter-bethe model where single MO for dominant fragment ions was assumed and assigned but the corresponding binding energy was substituted by the appearance potential for the particular ion fragment. The calculated values have been compared favorably with available experimental results. The sum of the fragment dissociation cross section improves the agreement between calculated values and experiment. Presented results demonstrate the increase of dominance of fragment ions with carbon bonds preserved in low-temperature laboratory plasma, due to their lower ionization threshold and higher absolute cross sections. Present empirical approach to the calculation is going to be further tested for more complex hydrocarbons.

ACKNOWLEDGMENTS

S. Popović gratefully acknowledges the support by the NRC/US Air Force Office of Scientific Research (AFOSR).

[1] C. Tian and C. R. Vidal, Chem. Phys. Lett. **288**, 499 (1998).
[2] C. Q. Jiao, C. A. DeJoseph, Jr., and A. Garscadden, J. Chem. Phys. **114**, 2166 (2001).
[3] W. Hwang, Y.-K. Kim, and M. E. Rudd, J. Chem. Phys. **104**, 2956 (1996).
[4] Y. K. Kim, W. Hwang, N. M. Weinberger, M. A. Ali, and M. E. Rudd, J. Chem. Phys. **106**, 1026 (1997).
[5] W. M. Huo, Phys. Rev. A **64**, 042719 (2001).
[6] http//physics.nist.gov/PhysRefData/Ionization/intro.html
[7] Y. K. Kim and M. E. Rudd, Phys. Rev. A **50**, 3954 (1994).
[8] M. J. Frisch, G. W. Trucks, H. B. Schlegel, G. E. Scuseria, M. A. Robb, J. R. Cheeseman, V. G. Zakrzewski, J. J. A. Montgomery, R. E. Stratmann, J. C. Burant, S. Dapprich, J. M. Millam, A. D. Daniels, K. N. Kudin, M. C. Strain, O. Farkas, J. Tomasi, V. Barone, M. Cossi, R. Cammi, B. Mennucci, C. Pomelli, C. Adamo, S. Clifford, J. Ochterski, G. A. Pétersson, P. Y. Ayala, Q. Cui, K. Morokuma, D. K. Malick, A. D. Rabuck, K. Raghavachari, J. B. Foresman, J. Cioslowski, J. V. Ortiz, B. B. Stefanov, G. Liu, A. Liashenko, P. Piskorz, I. Komaromi, R. Gomperts, R. L. Martin, D. J. Fox, T. Keith, M. A. Al-Laham, C. Y. Peng, A. Nanayakkara, C. Gonzalez, M. Challacombe, P. M. W. Gill, B. Johnson, W. Chen, M. W. Wong, J. L. Andres, C. Gonzalez, M. Head-Gordon, E. S. Replogle, and J. A. Pople, GAUSSIAN 98, vol. version A.9. (Gaussian, Inc., Pittsburgh, PA, 1998).
[9] P. Plessis and P. Marmet, Can. J. Phys. **65**, 165 (1986).
[10] D. Rapp and P. Englander-Golden, J. Chem. Phys. **43**, 1464 (1965).
[11] N. Nishimura and H. Tawara, J. Phys. B **27**, 2063 (1994).
[12] W. L. Fitch and A. D. Sauter, Anal. Chem. **55**, 832 (1983).